Electronic Supplementary Information (ESI) for

Nanoporous Networks as Caging Supports for Uniform, Surfactant-free Co_3O_4 Nanocrystals and Their Applications in Energy Storage and Conversion

Jeehye Byun, Hasmukh A. Patel, Dong Jun Kim, Chan Ho Jung, Jeong Young Park, Jang Wook Choi*, and Cafer T. Yavuz**

J. Byun, Dr. H. A. Patel, Prof. J. W. Choi, Prof. C. T. Yavuz
Graduate School of EEWS, Korea Advanced Institute of Science and Technology (KAIST), Daejeon 305-701, Republic of Korea
E-mail: yavuz@kaist.ac.kr, jangwookchoi@kaist.ac.kr

D. J. Kim
Department of Materials Science and Engineering, Korea Advanced Institute of Science and Technology (KAIST), Daejeon 305-701, Republic of Korea

C. H. Jung, Prof. J. Y. Park
Center for Nanomaterials and Chemical Reactions, Institute for Basic Science, Daejeon 305-701, Republic of Korea
E-mail: jeongypark@kaist.ac.kr

Keywords: Nanoporous covalent organic polymers, Nanocomposites, Lithium ion batteries, CO oxidation catalysts

TABLE OF CONTENTS

Figure S1. TEM images of (a) npCOP, (b) nwCOP, and (c) bare COP at a low magnification.

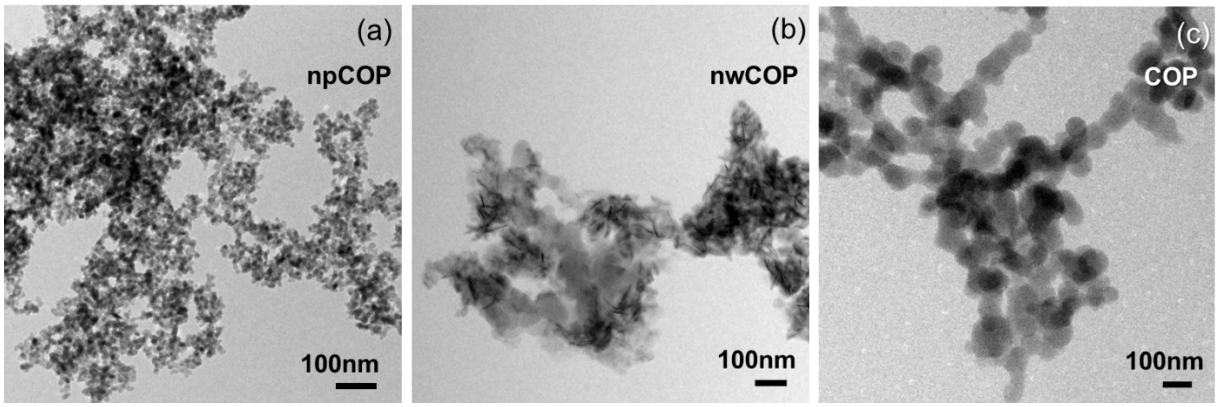

Figure S2. Morphology of Co_3O_4 nanoparticles templated by various amide porous polymers. The amine-terminated monomers, displayed as inset, are utilized instead of phenylene diamine in order to produce amide-linked porous polymers.

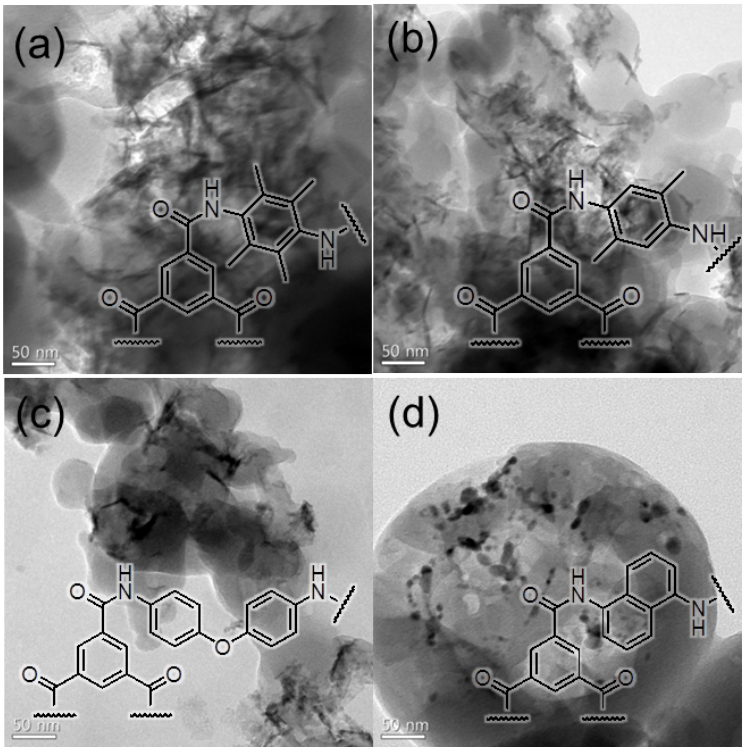

Figure S3. (a) XPS spectrum of npCOP and nwCOP, and (b) their Co 2p spectrum.

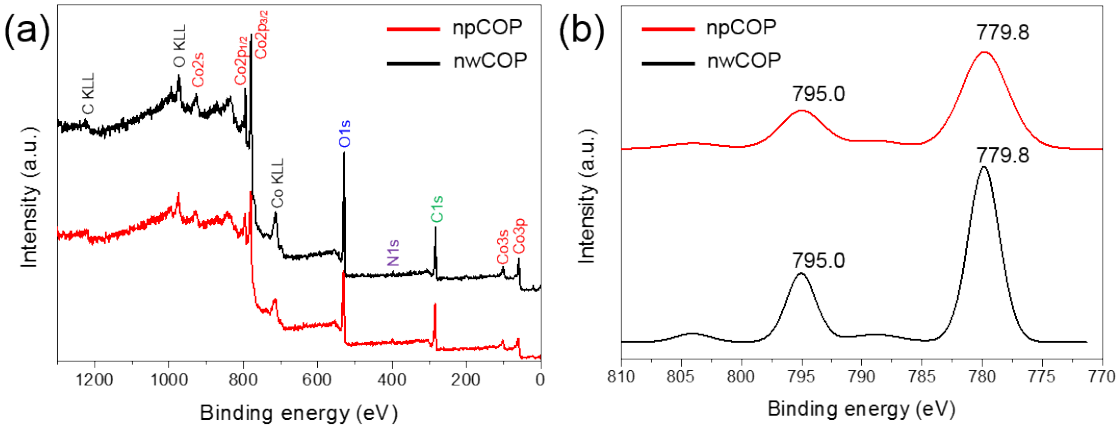

Figure S4. FTIR spectrum of bare COP and the nanocomposites with the range of stretching vibrations from metal-oxygen bonds.

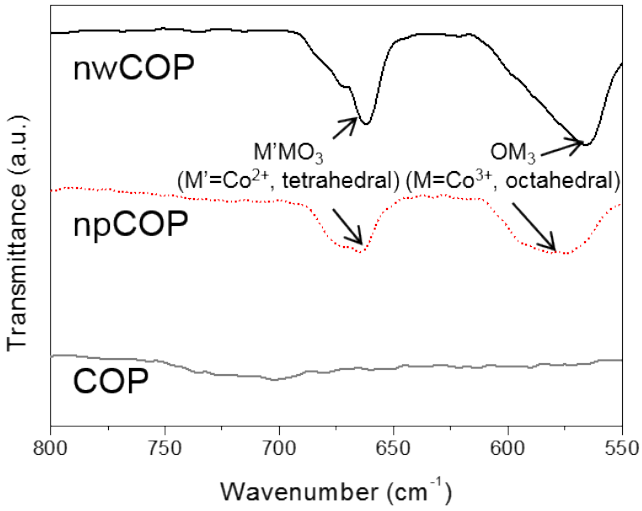

Figure S5. The first two galvanostatic cycles of (a) npCOP and (b) nwCOP with current density of 0.06 C (50 mA g^{-1}).

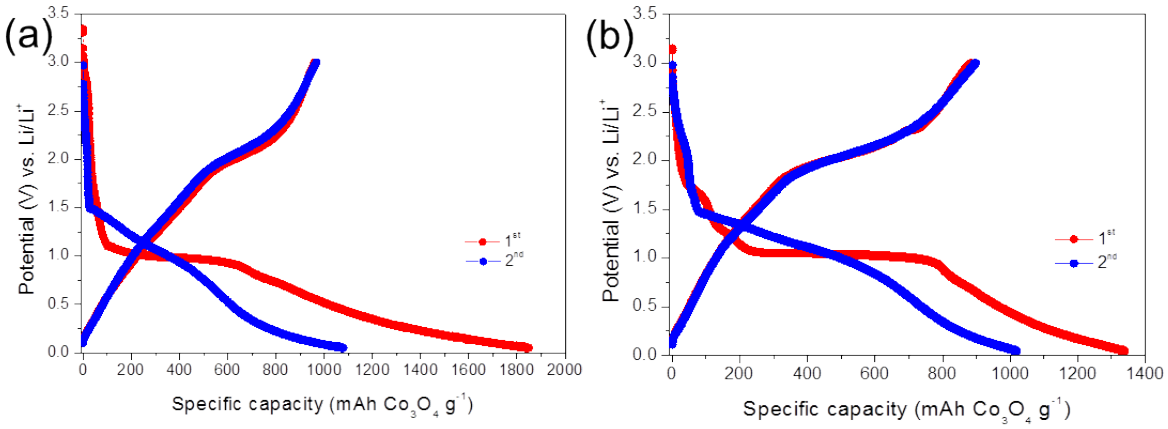

Figure S6. (a) Cyclic voltammograms of COP at a scanning rate of 200 μA s^{-1}. COP was pre-treated at 300 °C for accurate comparison with the nanocomposites. (b) Galvanostatic voltage profile of COP up to initial 5th cycle at current density of 0.06C (50 mA g^{-1}) (voltage range: 0.05 – 2 V). Cyclic voltammograms of (c) npCOP and (d) nwCOP at a scanning rate of 200 μA s^{-1}.

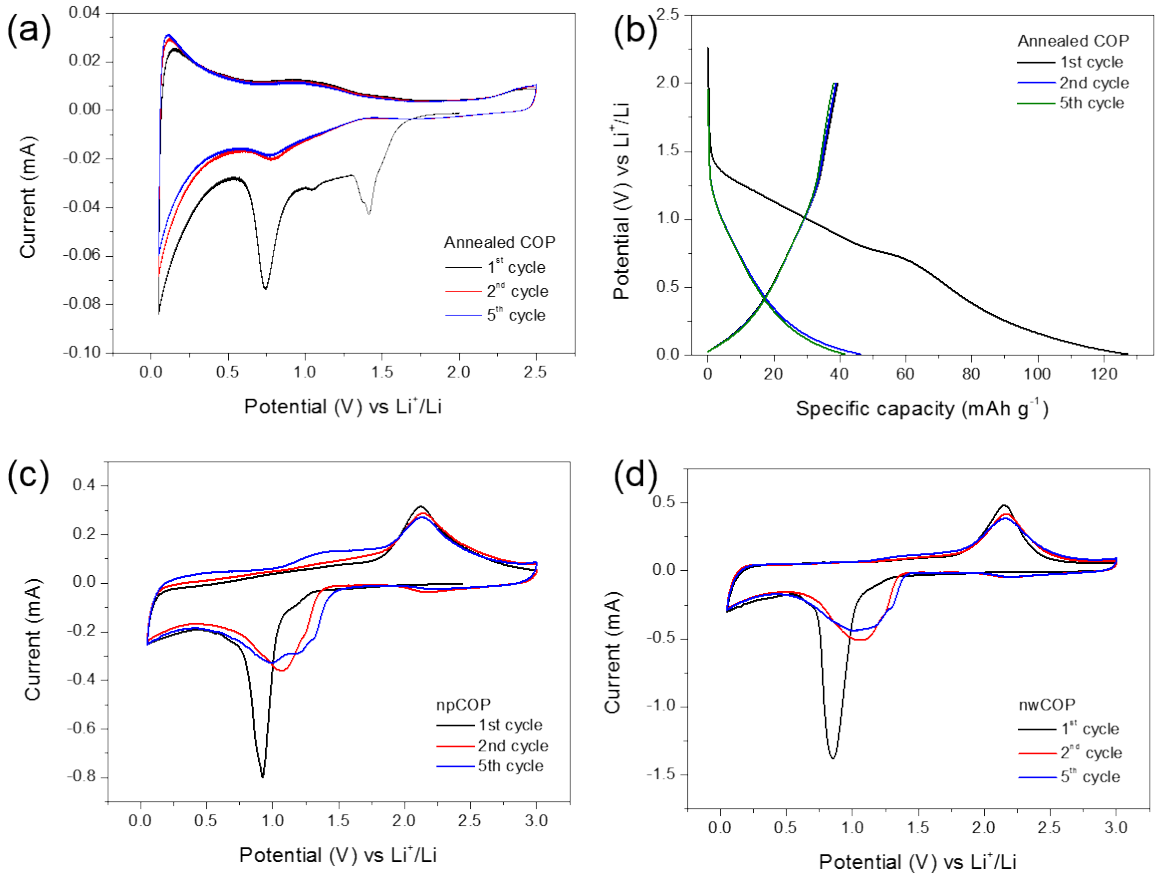

Figure S7. Rate performance of npCOP and nwCOP measured under different current densities.

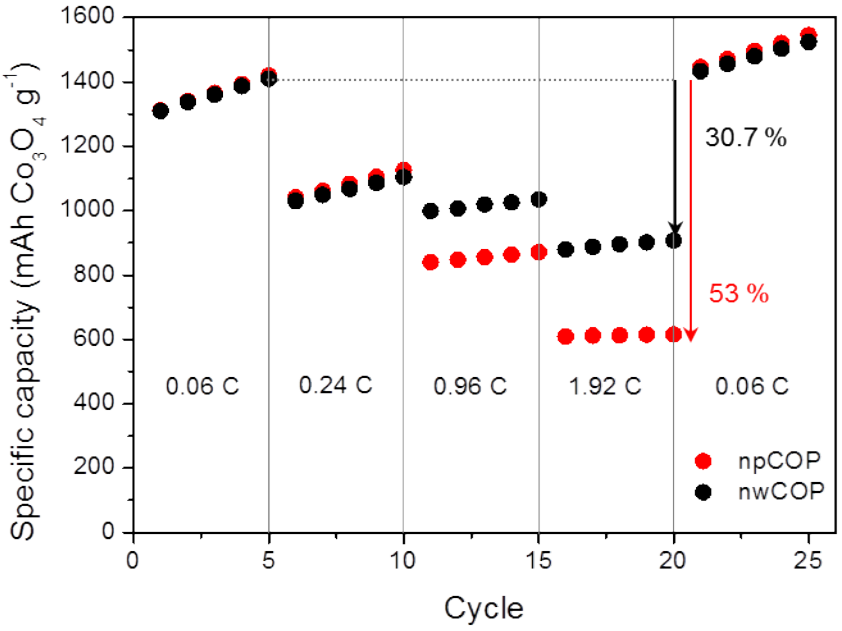

Figure S8. TEM morphology of (a) npCOP and (b) nwCOP after 60th cycle of charge-discharge. (c) Bare Co_3O_4 nanoparticles after a few cycles.

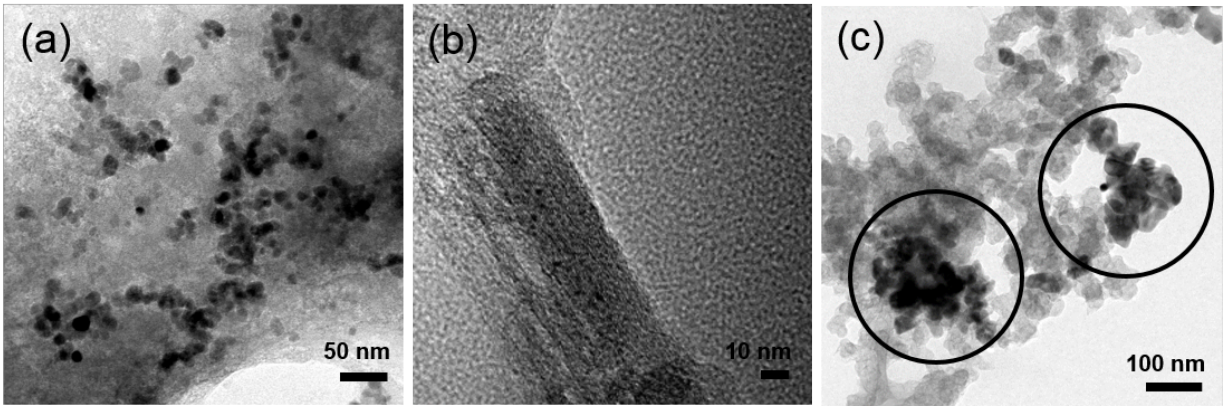

Figure S9. X-ray diffraction patterns of npCOP and nwCOP after 60 cycles.

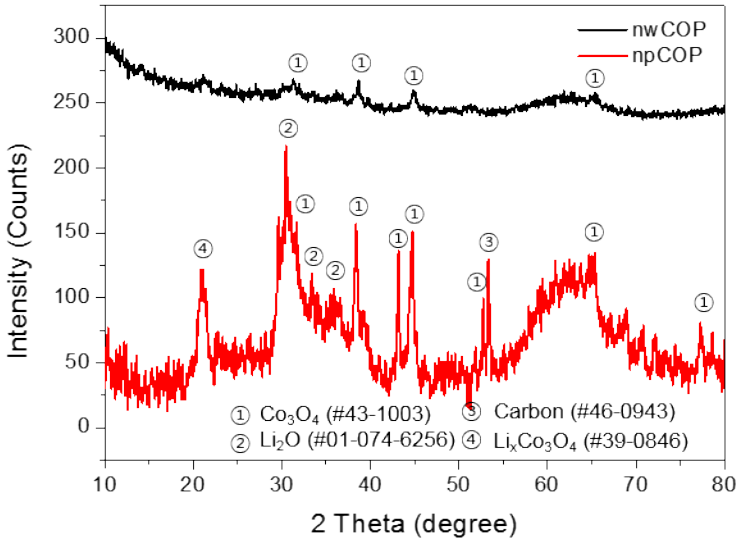

Figure S10. Thermogravimetric analysis of bare COP and the nanocomposites under (a) air and (b) N_2 atmosphere up to 800℃ at a rate of 10 ℃/min.

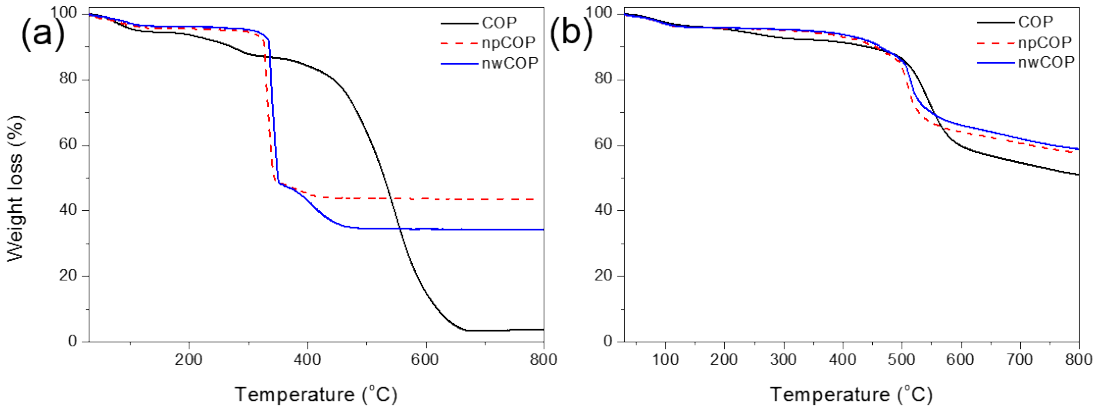

Figure S11. DRIFT spectrum obtained after exposure of the nanocomposites to carbon monoxide up to 120 ℃ for 37 h.

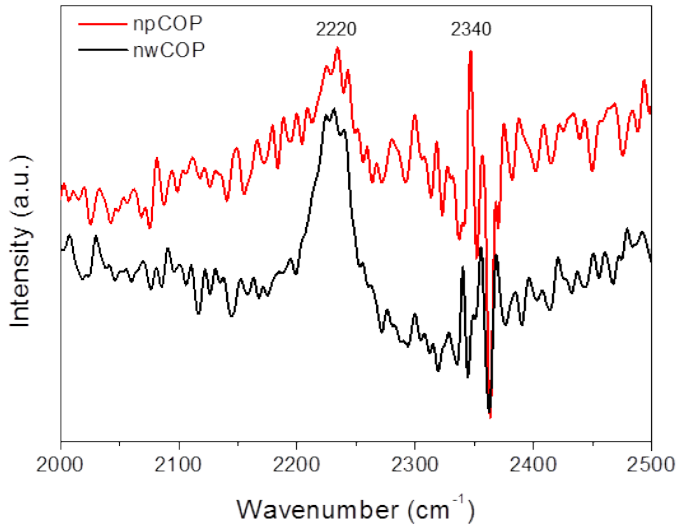

Table S1. Coulombic efficiency of npCOP and nwCOP in different cycles at 0.96C (1000 mA g^{-1}) and 1.92C (2000 mA g^{-1}) of current densities.

	npCOP	nwCOP	npCOP	nwCOP
Cycle	% @ 0.96C		% @ 1.92C	
1	51.03	72.40	51.12	71.79
2	88.90	91.37	88.25	92.98
3	92.27	92.48	91.95	93.98
10	95.90	95.77	95.69	95.86
61	96.53	94.06	96.92	95.51

Table S2. Structure and porosities of five new COPs introduced in this study. Please visit www.porouspolymers.com for a complete list of all COPs. (SA: Surface area)

	Structure	Porosity
COP-33 **Title 'COP' structure**	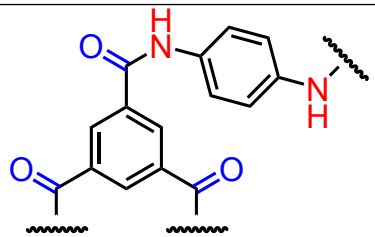	SA_{BET}: 53.2 m^2 g^{-1} $SA_{Langmuir}$: 73.4 m^2 g^{-1}
COP-43	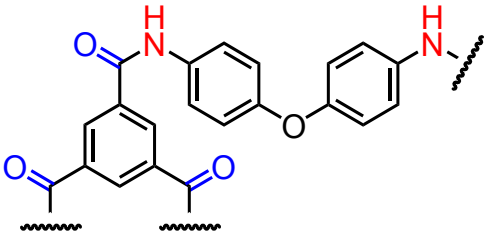	SA_{BET}: 33.3 m^2 g^{-1} $SA_{Langmuir}$: 45.8 m^2 g^{-1}
COP-45	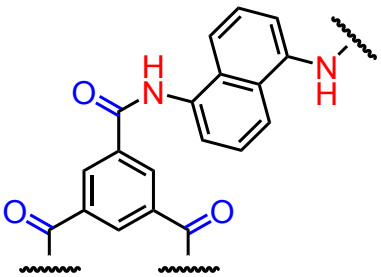	SA_{BET}: 16 m^2 g^{-1} $SA_{Langmuir}$: 22 m^2 g^{-1}
COP-58	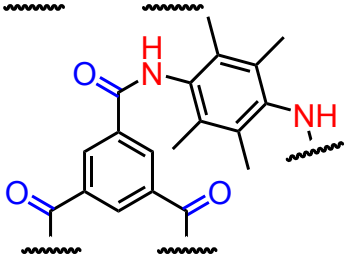	SA_{BET}: 15.3 m^2 g^{-1} $SA_{Langmuir}$: 20.1 m^2 g^{-1}
COP-59	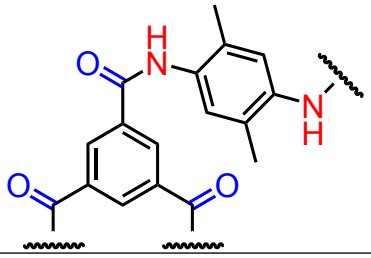	SA_{BET}: 39.3 m^2 g^{-1} $SA_{Langmuir}$: 53.7 m^2 g^{-1}

Table S3. Comparison of electrochemical performance with Co_3O_4-based materials.

Nanomaterial	Capacity [mAh g^{-1}]	C-rate	Cycle	References
Co_3O_4 hollow sphere	866	0.2 C	50	X. Wang et al. [1]
Mesoporous Co_3O_4	650	0.22 C	60	K. M. Shaju et al. [2]
Porous hollow Co_3O_4 nanosphere	820	0.11 C	100	D. Ge et al. [3]
Multilayered Co_3O_4 platelet	600	0.11 C	100	W. Yao et al. [4]
MON- Co_3O_4 composite	640	0.056 C	30	H. S. Lee et al. [5]
Co_3O_4 -porous polymer (npCOP)	980	0.96 C	60	**This study**

Table S4. CO oxidation catalytic activity and the reaction set-ups of cobalt oxide and its composite.

Nanomaterial	T_{100} [^oC]	Amount of catalyst (mg)	Gas flow rate (mL min^{-1})	Ratio between O_2 and CO	References
Co_3O_4-SiO_2	150	50	30	1% CO and 99% dry air	N. Yan et al. [6]
Co_3O_4-MOFs	150	100	50	1% CO and 20% O_2	W. Wang et al. [7]
Ordered mesoporous Co_3O_4	100	50	100	1% CO in air	S. Sun et al. [8]
Co_3O_4 particle	130	40	25	4% CO and 10% O_2	H. K. Lin et al. [9]
Porous Co_3O_4 microdisc	100	50	30	1% CO and 10% O_2	H. Che et al. [10]
Co_3O_4 nanobelt/cube	80	200	100	2.5% CO and 20% O_2	L. Hu et al. [11]
Co_3O_4 -porous polymer (npCOP)	100	100	50	4% CO and 10% O_2	**This study**

Supplementary References

1. Wang, X.; Wu, X. L.; Guo, Y. G.; Zhong, Y. T.; Cao, X. Q.; Ma, Y.; Yao, J. N., Synthesis and Lithium Storage Properties of Co_3O_4 Nanosheet-Assembled Multishelled Hollow Spheres. *Adv. Funct. Mater.* **2010,** *20* (10), 1680-1686.
2. Shaju, K. M.; Jiao, F.; Debart, A.; Bruce, P. G., Mesoporous and nanowire Co_3O_4 as negative electrodes for rechargeable lithium batteries. *Phys. Chem. Chem. Phys.* **2007,** *9* (15), 1837-1842.
3. Ge, D.; Geng, H.; Wang, J.; Zheng, J.; Pan, Y.; Cao, X.; Gu, H., Porous nano-structured Co_3O_4 anode materials generated from coordination-driven self-assembled aggregates for advanced lithium ion batteries. *Nanoscale* **2014,** *6* (16), 9689-9694.
4. Yao, W. L.; Yang, J.; Wang, J. L.; Nuli, Y., Multilayered Cobalt Oxide Platelets for Negative Electrode Material of a Lithium-Ion Battery. *J. Electrochem. Soc.* **2008,** *155* (12), A903-A908.
5. Lee, H. S.; Choi, J.; Jin, J.; Chun, J.; Lee, S. M.; Kim, H. J.; Son, S. U., An organometallic approach for microporous organic network (MON)- Co_3O_4 composites: enhanced stability as anode materials for lithium ion batteries. *Chem. Commun.* **2012,** *48* (1), 94-96.
6. Yan, N.; Chen, Q.; Wang, F.; Wang, Y.; Zhong, H.; Hu, L., High catalytic activity for CO oxidation of Co_3O_4 nanoparticles in SiO_2 nanocapsules. *J. Mater. Chem. A* **2013,** *1* (3), 637-643.
7. Wang, W. X.; Li, Y. W.; Zhang, R. J.; He, D. H.; Liu, H. L.; Liao, S. J., Metal-organic framework as a host for synthesis of nanoscale Co_3O_4 as an active catalyst for CO oxidation. *Catal. Commun.* **2011,** *12* (10), 875-879.
8. Sun, S. J.; Gao, Q. M.; Wang, H. L.; Zhu, J. K.; Guo, H. L., Influence of textural parameters on the catalytic behavior for CO oxidation over ordered mesoporous Co_3O_4. *Appl. Catal., B* **2010,** *97* (1-2), 284-291.
9. Lin, H. K.; Chiu, H. C.; Tsai, H. C.; Chien, S. H.; Wang, C. B., Synthesis, characterization and catalytic oxidation of carbon monoxide over cobalt oxide. *Catal. Lett.* **2003,** *88* (3-4), 169-174.
10. Che, H. W.; Liu, A. F.; Fu, Q. R.; Jiang, R. J., Facile synthesis of porous cobalt oxide microdiscs and their catalytic property in CO oxidation. *Mater. Lett.* **2013,** *93*, 240-242.
11. Hu, L. H.; Sun, K. Q.; Peng, Q.; Xu, B. Q.; Li, Y. D., Surface Active Sites on Co_3O_4 Nanobelt and Nanocube Model Catalysts for CO Oxidation. *Nano Res.* **2010,** *3* (5), 363-368.